

Probing the flow-induced shish-kebab structure in entangled polyethylene melts by synchrotron X-ray scattering

Jong Kahk Keum, Feng Zuo and Benjamin S. Hsiao*

Department of Chemistry, Stony Brook University, Stony Brook, NY 11794-3400, USA. Correspondence e-mail: bhsiao@notes.cc.sunysb.edu

Received 16 August 2006
Accepted 15 November 2006

In-situ rheo small-angle X-ray scattering (SAXS) and rheo wide-angle X-ray diffraction (WAXD) techniques were used to investigate the flow-induced crystalline structure in entangled melts of ultrahigh-molecular-weight polyethylene (UHMWPE)/low-molecular-weight polyethylene (LMWPE) blends (0, 2 and 5 wt% of UHMWPE). Immediately after a step shear at 415 K, SAXS and WAXD results confirmed that only the shish structure was formed in the melts without kebabs. The topological deformation of entangled UHMWPE chains in the blend was responsible for the formation of shish. The missing kebab growth in the presence of shish indicated that secondary nucleation of coiled chains on the shish surface was frustrated at high temperatures close to the equilibrium melting temperature (418.5 K). When the temperature was quenched to 407 K, both blends (but not pure LMWPE) clearly exhibited oriented kebab growth. An Avrami analysis was applied to investigate the nucleation and growth of kebabs. Results indicated that kebabs were probably grown under athermal nucleation and diffusion-controlled conditions. In addition, the crystallization rate under predetermined nucleation was strongly governed by the concentration of shish.

© 2007 International Union of Crystallography
Printed in Great Britain – all rights reserved

1. Introduction

Prior to crystallization, the initially formed flow-induced crystallization precursor structure (shish), with a molecular orientation induced by flow during polymer processing – such as extrusion, injection molding, fiber spinning, and film blowing – can often dictate the subsequent morphology and, thus, the final properties of the polymer (Hill & Keller, 1969; Keller, 1979; Dukovski & Muthukumar, 2003; Hsiao *et al.*, 2005; Keum *et al.*, 2005). Although extensive research on flow-induced crystallization has been conducted, the nature of the earliest event (*i.e.*, flow-induced crystallization precursor structure formation), prior to the full-scale crystallization under flow, is still not fully understood. It is thought that the topological deformation of highly entangled polymer chains under flow and their evolution into extended-chain crystal (shish) directly affect the subsequent developments of kebab (folded-chain lamella) as well as the final morphology of polymer products (Zuo *et al.*, 2006).

Recent experimental studies verify that the high-molecular-weight tail in the molecular weight distribution plays a critical role in the formation of the initial crystallization precursor structure in an entangled polymer melt under a given flow condition (Somani *et al.*, 2000; Seki *et al.*, 2002; Keum *et al.*, 2005; Zuo *et al.*, 2006). The molecular basis of flow-induced shish-kebab formation in entangled melts is primarily based on the concept of coil-stretch transition of polymer chains in dilute solutions first proposed by de Gennes (de Gennes, 1974). It is Keller and Kolnaar who introduced the concept of coil-stretch transition into entangled polymer melts, whereby they proposed the existence of a critical orientation molecular weight, M^* , of linear polymer chain that can be scaled with critical strain,

$\dot{\epsilon}_c \simeq (M^*)^{-\beta}$ (Keller & Kolnaar, 1993). That is, depending on the molecular weight, only polymer chains with molecular weights higher than M^* can remain stretched after a given flow, while shorter chains relax back into the coiled state. We recently reported on the nature of shish-kebab formation in highly entangled polymer melts (Zuo *et al.*, 2006). We argued that highly entangled chains with molecular weight higher than M^* in a supercooled melt could form a stretched entanglement network after shear, under the assumption that the full scale of chain disentanglement could not occur under typical flow conditions. Namely, the interplay between the deformation field and the high-molecular-weight species are mainly responsible for the formation of shish.

In this study, a unique polymer blend system was used to simulate the formation of the precursor structures at the initial stage of flow-induced crystallization. In these blends, a low-molecular-weight polyethylene (LMWPE) was used as the matrix material and an ultrahigh-molecular-weight polyethylene (UHMWPE) that is miscible with LMWPE at low concentrations was used as the nucleating minor component.

2. Experimental

2.1. Materials and sample preparation

Two distinctively different polyethylene samples (UHMWPE and LMWPE) with well separated relaxation spectra were chosen to prepare the blends. Both LMWPE (average molecular weight, $\bar{M}_w = 110\,000\text{ g mol}^{-1}$ and polydispersity = 9) and UHMWPE samples ($\bar{M}_w = 5\,500\,000\text{ g mol}^{-1}$, polydispersity = 9) were polymerized using

Ziegler–Natta catalysts. The chosen concentrations of UHMWPE in LMWPE were 2 and 5 wt%, which were significantly higher than the overlap concentration of UHMWPE, c^* ($= 0.2$ wt%). The overlap concentration was calculated based on the equation $c^* = 3M_w/4\pi[\langle R_g^2 \rangle^{1/2}]^3 N_a$, $\langle R_g^2 \rangle^{1/2}$ being the root-mean-square radius of gyration and N_a being Avogadro's number (de Gennes, 1979; Takahashi *et al.*, 1985; Yang *et al.*, 2004). The characteristic ratio of $\langle R_g^2 \rangle^{1/2} / \bar{M}_w^{1/2}$ was 0.46 based on small-angle neutron scattering (SANS) measurements (Fetters *et al.*, 2002). The polymer blends were prepared by a solution-mixing procedure to ensure the thorough blending of the two different species at the molecular level. To prevent sample degradation during mixing, 3 wt% of Igornox 1076 was added. The detailed mixing procedure has been illustrated elsewhere (Yang *et al.*, 2004). Polymer films with about 0.5 mm thickness were prepared by compression molding at 445 K for 5 min. Samples in the form of a ring (inner diameter = 10 mm, outer diameter = 20 mm) were cut from the melt-pressed films for X-ray measurements.

2.2. Synchrotron X-ray characterization

A Linkam CSS-450 optical shear stage, modified for *in-situ* rheo-X-ray studies was used to apply controlled shear conditions to the polymer melts. The details of this modified shear apparatus have been described elsewhere (Somani *et al.*, 2000). *In-situ* rheo small-angle X-ray scattering (rheo-SAXS) and rheo wide-angle X-ray diffraction (rheo-WAXD) measurements were carried out at the X27C beamline at the National Synchrotron Light Source (NSLS), Brookhaven National Laboratory (BNL). The wavelength of the synchrotron radiation used was 1.371 Å. Two-dimensional SAXS/WAXD patterns were collected by using a MAR CCD X-ray detector (MAR-USA), which had a resolution of 1024×1024 pixels (pixel size = $158.44 \mu\text{m}$). For SAXS and WAXD measurements, the sample-to-detector distances were 1832 and 112.4 mm. All X-ray patterns (SAXS and WAXD) were corrected for background scattering, air scattering, sample absorption and beam-intensity fluctuations.

2.3. Experimental procedures

In order to ensure that the polymer melts were free of any memory effects associated with the prior thermal and mechanical history, all polymer samples were first subjected to a heating scan to 445 K, which is substantially higher than the theoretical equilibrium melting temperature of polyethylene ($T_m^0 \approx 418.5$ K), and were held there for 5 min. The melts were then cooled down to the chosen crystallization temperature (*i.e.*, 415 K) at a rate of -30 K min^{-1} . The chosen shear conditions were shear rate $\dot{\gamma} = 100 \text{ s}^{-1}$, shear duration $\gamma_s = 5$ s. When the temperature reached the chosen experimental temperature

(415 K), SAXS and WAXD images were collected in real time. The data-acquisition time for both SAXS and WAXD was 15 s and the data-storage time was 5 s per pattern. After 45 min at the isothermal condition after shear, the once-sheared melts were quenched to 407 K and maintained for 30 min to investigate the subsequent crystallization behavior.

3. Results and discussions

3.1. Flow-induced shish formation at 415 K

Fig. 1 illustrates selected rheo-SAXS patterns of pure LMWPE and UHMWPE/LMWPE blends collected after 35 s of step shear at 415 K. Before shear, all melts showed only diffuse scattering features, indicating that all melts were in the amorphous state. Immediately after shear, strong equatorial streaks were seen only in the blends (Fig. 1*b* and *c*), suggesting the formation of a large-scale ordered structure, *i.e.*, shish. In contrast, the sheared pure LMWPE melt only exhibited amorphous scattering features (Fig. 1*a*) and subsequent crystallization at temperatures of 410 and 404 K did not change the pattern. This confirmed that shish was not formed in LMWPE after shear at the experimental conditions and all deformed chains relaxed back to the coiled states. The appearance of the equatorial streaks in the blends can be attributed to the shear-induced crystallization of the UHMWPE component because of its very long relaxation time $\tau \propto M^{3.4}$ (M represents the molecular weight).

It is interesting to note that even though both blends clearly exhibited the evolution of shish, no kebab evolution (in the form of meridional scattering peaks or scattering gain) was observed (Fig. 1*b* and *c*). It has been proposed that the nucleation of kebabs on the surface of shish involves the adsorption of coiled chains (or segments) (Dukovski & Muthukumar, 2003). It is conceivable that when the experimental temperature (415 K) is near the equilibrium melting temperature (418.5 K), the high thermal motion of the chain will prevent its adsorption to the shish surface and the initiation of the kebab growth. In addition, thermodynamically speaking, when the temperature is near the equilibrium melting temperature, the coiled chains would encounter a very high nucleation barrier for the formation of folded-chain lamellae.

Rheo-WAXD patterns for each melt collected after 35 s of shear at conditions identical to those of the SAXS study are shown in Fig. 2. Highly oriented equatorial 110 crystalline reflections appeared in the WAXD patterns of blends but not in pure LMWPE, which confirmed the shish formation observed in SAXS patterns. The observation indicates that the shish structure consists of extended-chain crystals.

The shish structure was found to relax first after the cessation of shear but grow subsequently. In order to investigate the evolution of

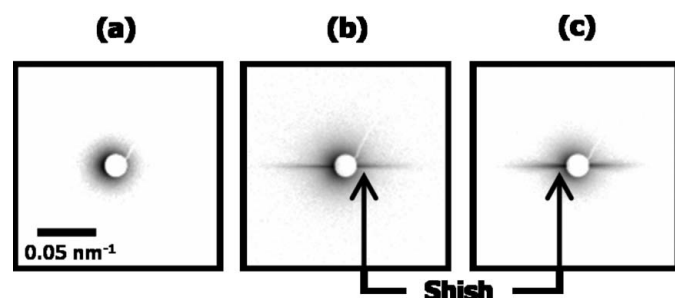


Figure 1
Selected rheo-SAXS patterns of (a) pure LMWPE, (b) 2/98 (UHMWPE/LMWPE) blend and (c) 5/95 blend, collected at 35 s after step shear at 415 K; shear rate $\dot{\gamma} = 100 \text{ s}^{-1}$ and shear duration $\gamma_s = 5$ s. The flow axis is vertical.

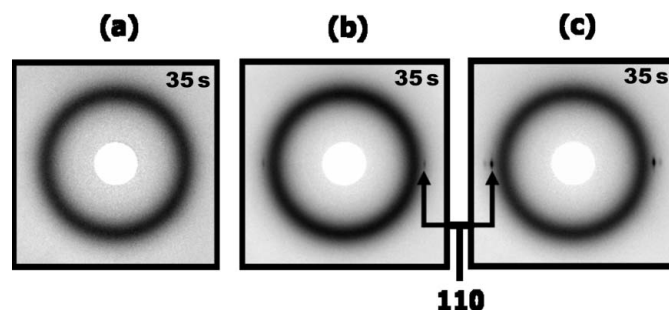


Figure 2
Rheo-WAXD patterns of (a) pure LMWPE, (b) 2/98 blend and (c) 5/95 blend obtained at 35 s after step shear at 415 K; shear rate $\dot{\gamma} = 100 \text{ s}^{-1}$ and shear duration $\gamma_s = 5$ s. The flow axis is vertical.

Table 1

Avrami exponent (n) and constant (k) estimated from the WAXD data due to the kebab growth.

	n	k
2/98 UHMWPE/HDPE blend	1.1	3.1
5/95 UHMWPE/HDPE blend	1.2	19.1

shish, the scattering intensity from the shish, $I_{\text{Shish}}(s, \phi)$, was determined from the rheo-SAXS data. This value can be calculated by $I_{\text{Shish}}(s, \phi) = 4\pi \int_{0.0087}^{0.31} \int_{-20^\circ}^{+20^\circ} I(s, \phi) ds d\phi$, where s is the modulus of the scattering vector ($s = 2 \sin \theta / \lambda$, where θ and λ are the scattering angle and X-ray beam wavelength) and ϕ is the azimuthal angle. The evolution of scattering intensity from shish for the blends is depicted as a function of crystallization time in Fig. 3. The changes may be divided into two stages: an initial decrease at $t < 400$ s and a subsequent increase at $t > 400$ s. The 5/95 (UHMWPE/LMWPE) blend exhibited higher scattering intensity than the 2/98 blend over the entire time period. Since the scattering intensity, $I_{\text{Shish}}(s, \phi)$, is proportional to the volume of shish, v , it is thought that a higher volume fraction of shish was formed in the 5/95 blend due to higher concentration of UHMWPE.

Immediately after shear, the initial decrease in the shish intensity at $t > 400$ s indicates that the volume fraction of shish began to fall. This is because when the applied shear was removed, the stretched chain segments between the entanglements could relax back to the coiled state. However, this value increased at a time greater than 400 s, which implied the growth of shish. The growth mechanism is probably mediated by crystallization of some partially deformed/oriented UHMWPE chains.

3.2. Flow-induced kebab formation at 407 K

After holding at 415 K for 45 min, the once-sheared melts were cooled to 407 K to investigate the subsequent crystallization behavior. Selected rheo-SAXS patterns obtained from the blends immediately after cooling (at a rate of -30 K min^{-1}) are shown in Fig. 4. The pure LMWPE exhibited only diffuse scattering features, whereas

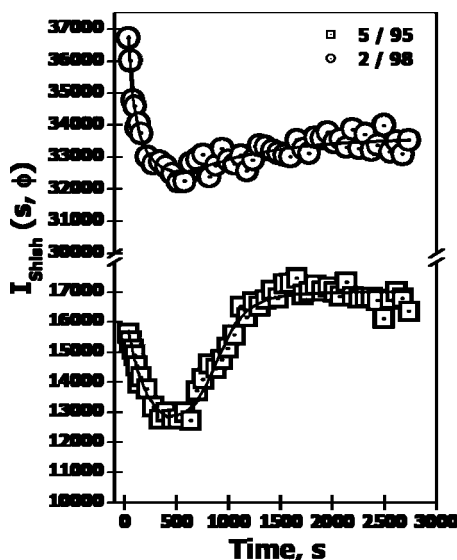


Figure 3
The changes of scattering intensity during shish evolution in 5/95 blend and 2/98 blend. The scattering intensity of shish, $I_{\text{Shish}}(s, \phi)$, was extracted from rheo-SAXS patterns as partly shown in Fig. 1.

the blends clearly showed the emergence of two scattering maxima on the meridian superimposed on the equatorial streaks formed at 415 K. The occurrence of meridional peaks indicates the formation of kebabs (or folded-chain lamellae), which were stacked perpendicularly along the flow direction. The 5/95 blend shows stronger scattering intensity from kebabs than the 2/98 blend.

In order to investigate the nucleation and growth of kebabs, a simplified Avrami analysis using equation (1) was applied (Avrami, 1939; Gedde, 1995).

$$\frac{v_c(t)}{v_c(\infty)} = 1 - \exp(-Kt^n) \quad (1)$$

where, $v_c(t)$ and $v_c(\infty)$ are volume fractions of kebab crystals at time t and at infinity, respectively. K and n are the rate constant and Avrami exponent, respectively. We further assume the following two relations: (1) $v_c(t)/v_c(\infty) \simeq V \simeq I_c(t)/I_c(\infty) \simeq I_c(t)$, and (2) $\exp(-Kt^n) \simeq 1 - Kt^n + \dots$, where $I_c(t)$ and $I_c(\infty)$ are reflected intensities of crystal at time t and infinity, respectively. This approximation allows one to simplify the Avrami equation,

$$I_c(t) \simeq kt^n \quad (2)$$

Thus based on the changes in 110 intensity from the WAXD patterns, the Avrami exponent (n) and constant (k), which is related to the rate constant (K), were obtained using equation (2) and the results are shown in Table 1. It was found that the estimated Avrami exponents for both blends at the initial stage of kebab formation are about unity. This is consistent with the previous hypothesis that the two-dimensional kebabs grow under athermal nucleation and diffusion-controlled conditions (Hsiao *et al.*, 2005). The large difference in the constant k , which is related to the crystallization rate, implied that the rate of kebab growth was much faster in the 5/95 blend than the 2/98 blend under the same nucleation and growth regimes.

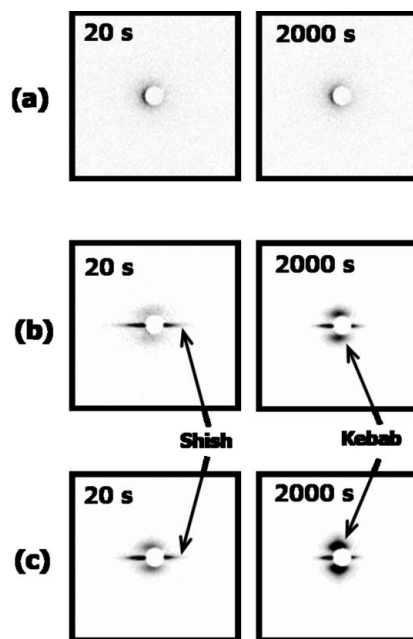


Figure 4
Selected rheo-two-dimensional SAXS patterns of (a) pure LMWPE, (b) 2/98 blend and (c) 5/95 blend collected immediately after cooling from 415 to 407 K. The shish axis is vertical.

4. Conclusions

Rheo-SAXS and rheo-WAXD studies of UHMWPE/LMWPE blends near the equilibrium melting temperature of polyethylene confirmed that the formation of shish originated from UHMWPE chains. The deformed chains under shear generate a deformed entanglement network, where the stretched chain segments between the entanglement points undergo crystallization and form shish. After shear, the shish content decreases initially due to the relaxation of the deformed network, but increases later due to the nucleation and growth behavior. As temperature decreased to 407 K, both blends (but not pure LMWPE) indicated the formation of oriented kebabs. The Avrami analysis based on the WAXD data confirmed that the growth of kebab was diffusion-controlled rather than nucleation-controlled, under athermal nucleation. The kebab growth rate in the 5/95 blend was much faster than that in the 2/98 blend. The growth rate of kebab was strongly influenced by the concentration of shish.

The authors acknowledge the assistance of Drs Igors Sics and Lixia Rong in the synchrotron SAXS and WAXD experimental setup. Financial support for this work was provided by the National Science Foundation (DMR-0405432).

References

- Avrami, M. (1939). *J. Chem. Phys.* **7**, 1103–1112.
- Dukovski, I. & Muthukumar, M. (2003). *J. Chem. Phys.* **118**, 6648–6655.
- Fetters, L. J., Lohse, D. J., Garcia-Franco, C. A., Brant, P. & Richter, D. (2002). *Macromolecules*, **35**, 10096–10101.
- Gedde, U. W. (1995). *Polymer Physics*. New York: Chapman and Hall.
- Gennes, P. G. de (1974). *J. Chem. Phys.* **60**, 5030–5042.
- Gennes, P. G. de (1979). *Scaling Concepts in Polymer Physics*. Ithaca, NY: Cornell University Press.
- Hill, M. J. & Keller, A. (1969). *J. Macromol. Sci. Phys. B.* **3**, 153–169.
- Hsiao, B. S., Yang, L., Somani, R. H., Carlos, A. A. & Zhu, L. (2005). *Phys. Rev. Lett.* **94**, 117802-1–117802-4.
- Keller, A. (1979). *Faraday Discuss. R. Soc. Chem.* **68**, 145–166.
- Keller, A. & Kolnaar, J. W. H. (1993). *Prog. Colloid. Polym. Sci.* **92**, 81–102.
- Keum, J. K., Burger, C., Hsiao, B. S., Somani, R. H., Yang, L., Chu, B., Kolb, R., Chen, H. & Lue, C. (2005). *Prog. Colloid. Polym. Sci.* **130**, 114–126.
- Seki, M., Thurman, D. W., Oberhauser, J. P. & Kornfield, J. A. (2002). *Macromolecules*, **35**, 2583–2594.
- Somani, R. H., Hsiao, B. S., Nogales, A., Srinivas, S., Tsou, A. H., Sics, I., Balta Calleja, F. J. & Ezquerra, T. A. (2000). *Macromolecules*, **33**, 9385–9394.
- Takahashi, Y., Isono, Y., Noda, I. & Nagasawa, M. (1985). *Macromolecules*, **18**, 1002–1008.
- Yang, L., Somani, R. H., Sics, I., Hsiao, B. S., Kolb, R., Fruitwala, H. & Ong, C. (2004). *Macromolecules*, **37**, 4845–4859.
- Zuo, F., Keum, J. K., Yang, L., Somani, R. H. & Hsiao, B. S. (2006). *Macromolecules*, **39**, 2209–2218.